Deltex-1 mutations predict poor survival in diffuse large B-cell lymphoma

Leo Meriranta,[1,2] Annika Pasanen,[1,2] Riku Louhimo,[1] Alejandra Cervera,[1] Amjad Alkodsi,[1] Matias Autio,[1,2] Minna Taskinen,[1,2] Ville Rantanen,[1] Marja-Liisa Karjalainen-Lindsberg,[3] Harald Holte,[4] Jan Delabie,[5,6] Rainer Lehtonen,[1] Sampsa Hautaniemi[1] and Sirpa Leppä[1,2]

[1]Research Programs Unit, Genome-Scale Biology Program, Faculty of Medicine, University of Helsinki, Finland; [2]Department of Oncology, Helsinki University Hospital Comprehensive Cancer Center, Finland; [3]Department of Pathology, Helsinki University Hospital, Finland; [4]Department of Oncology, Oslo University Hospital, Norway; [5]Department of Pathology, University of Toronto, ON, Canada, and [6]Department of Pathology, Oslo University Hospital, Norway

Correspondence: sirpa.leppa@helsinki.fi
doi:10.3324/haematol.2016.157495

Supplementary Material

Deltex-1 mutations predict poor survival in diffuse large B-cell lymphoma

Leo Meriranta[1,2], Annika Pasanen[1,2], Riku Louhimo[1], Alejandra Cervera[1], Amjad Alkodsi [1], Matias Autio[1,2], Minna Taskinen[1,2], Ville Rantanen[1], Marja-Liisa Karjalainen-Lindsberg[3], Harald Holte[4], Jan Delabie[5], Rainer Lehtonen[1], Sampsa Hautaniemi[1], and Sirpa Leppä[1,2]

[1]Research Programs Unit, Genome Scale Biology Program, Faculty of Medicine, University of Helsinki, Helsinki, Finland; [2]Department of Oncology, Helsinki University Central Hospital Cancer Center, Helsinki, Finland; [3]Department of Pathology, Helsinki University Hospital, Helsinki, Finland, [4]Department of Oncology, Oslo University Hospital, Oslo, Norway; [5]Department of Pathology, University of Toronto, Canada, and Department of Pathology, Oslo University Hospital, Oslo, Norway

Supplementary Methods

Patients

Initial screening cohort consisted of eight clinically high risk DLBCL patients with age adjusted International Prognostic Index (aaIPI) Score 2 or 3. The patients were treated according to a Nordic phase II NLG-LBC-04 protocol with six courses of R-CHOEP14 regimen (rituximab, cyclophosphamide, doxorubicin, vincristine, etoposide, and prednisone) supported with G-CSF followed by systemic CNS prophylaxis with one course of high-dose methotrexate and one course of high-dose cytarabine (1). Sample selection was based on the availability of fresh frozen tissue for DNA extraction and exome sequencing.

Discovery cohort consisted of 92 DLBCL patients with clinical and RNA sequencing data generated by National Cancer Institute (NCI) Cancer Genome Characterization Initiative (CGCI; dbGaP database applied study accession: phs000532.v3.p1) (2, 3). The patients were treated with R-CHOP-like regimen.

Nordic validation cohort consisted of 145 DLBCL patients. Of these, 52 patients were treated in a Nordic NLG-LBC-04 protocol (LBC-04 expansion) (1). Additional 93 patients were treated with R-CHOP-like therapy at the Helsinki University Hospital Cancer Center (independent 'Nordic' patient cohort). Sample selection was based on the availability of fresh frozen or formalin fixed paraffin embedded (FFPE) tissue for DNA extraction and Sanger sequencing, and immunohistochemistry. In addition, oligonucleotide-based microarray from 233

DLBCL patients generated by the Lymphoma/Leukemia Molecular Profiling Project (LLMPP; GEO dataset: GSE10846) was used for validation (4).

Ethics statement

The study was approved by the National Authority for Medicolegal Affairs, Finland, and Institutional Review Board, and Ethics Committees in Helsinki, Finland. Written informed consent was obtained prior to treatment and sampling from all patients included in the NLG-LBC-04 study. Protocol and sampling were approved by the relevant authorities in the participating countries. The trial was registered at ClinicalTrials.gov, number NCT01502982.

DNA isolation

Tumor DNA for the initial screening cohort was extracted from fresh frozen tissue of primary DLBCL samples with AllPrep DNA/RNA/Protein Mini kit (Qiaqen, Hilden, Germany), and matched normal DNA derived from peripheral blood leukocytes with Nucleospin Blood L kit (Macherey-Nagel, Düren, Germany) according to manufacturer's instructions. For the validation cohort, fresh frozen tissue or two or three 20 µM sections were cut from the FFPE blocks and processed according to the manufacturer's protocol. DNAs from FFPE tissue were isolated with QiAmp DNA FFPE Tissue kit (Qiagen).

Whole-exome sequencing

Exome capture was performed using the Nimblegen SeqCap EZ v2.0 capture Kit (Roche NimbleGen, Madison, WI), and sequencing of exomes performed using HiSeq1500 instrument (Illumina, San Diego. CA). Short-reads from tumors were aligned to the human reference genome with bwa (5) and duplicates removed with samtools (6). Variants were called with VarScan version 2.3.6 (somatic *p-value =0.05*, strand-filter=1, minimum of 20% reads report variant allele) (7). Functional effects of SNVs were annotated with Annovar (8). Only variants that mapped within 2 bp of known exon boundaries were included in further analyses. Moreover, SNVs that coincided with known germline variants in the 1000 Genomes or dbSnp data sets were removed. Manual review of sequencing alignments was performed with Integrative Genomics Viewer v2.3.6 (Broadinstitute; http://www.broadinstitute.org/igv/).

CGCI variant filtering and identification of survival-associated genes

From the original CGCI cohort consisting of 97 patients with de novo DLBCL with molecular subtype information, RNA-seq and clinical data, 92 patients that had been treated with R-CHOP-like regimen were selected for the analyses. The raw sequencing files were assessed for quality with FastQC (9) and adaptors and low-

quality bases (<20 phred score) were trimmed with Trimmomatic (10). The reads were aligned to GRCh37 (hg19) using TopHat (11) and expression was quantified with Cufflinks (12). Bambino (13) was used for variant calling using only the reads with unique alignments and a maximum of three mismatches per read. Variants next to the stretches of four repeated nucleotides and variants not covered by at least three reads and consisting of at least 10% of the tumor were discarded. Annovar (8) was used for functional annotation. Non-disease associated known polymorphisms were removed. When CADD scoring (14) was implemented, only the variants with no available score, or scaled score of at least 10 were kept. Finally, for the survival analysis, only the genes that were also found to have variations in the exome sequencing samples were selected. Univariate association between mutated and non-mutated samples for progression free survival (PFS) and overall survival (OS) was tested using the log-rank test.

Sanger sequencing of WWE1-domain in *DTX1*

Polymerase chain reaction (PCR) was performed using specific primers designed with Primer-BLAST for exons 1 and 2 of the *DTX1* WWE1-domain. PCR products were purified with ExoSAP-IT (Affymetrix, Santa Clara, CA) according to manufacturer's instructions and subjected to Sanger sequencing on both strands using BigDye v1.1 Cycle Sequencing kit and the ABI PRISM 3730xl DNA analyzer at the FIMM. Primer details and PCR conditions are available on request. Mutations were detected using Mutation Surveyor software v4.0.9 (Softgenetics, State College, PA) and FinchTV v1.4.0 (Geospiza Inc, Seattle, WA). Non-disease associated known polymorphisms were removed using MutationTaster (15).

Immunohistochemistry

Immunohistochemical staining of Deltex-1 was performed on FFPE tissue sections on whole tissue slides. Of the Deltex-1 antibodies tested, MAB7157 (R&D Systems, MN, USA) was selected based on its ability to recognize HA-tagged Deltex-1 expressed in 293T cells. After deparaffination, heat-induced epitope retrieval (121°C, 3 min), and blocking of endogenous peroxidase, the slides were incubated with anti-Deltex-1 antibody (1:100) at 4°C overnight. Staining was completed with Vectastain ABC kit reagents (Vector Laboratories, Burlingame, CA) according to the manufacturer's instructions, and slides were counterstained with hematoxylin.

To score the stainings, Deltex-1-positivity was evaluated from one to three high-power fields (hpf; x630 magnification) with the Leica DM LB bright-field microscope (Leica Microsystems GmbH) and a camera attached to it (Olympus DP50, InStudio 1.0.1 Software). The most representative areas with intense staining pattern were

first selected with low magnification and further digitized with hpf, resulting in microscopic images with area size of 0.02 mm^2. Images were subsequently scored using computerized image analysis system Anim (16). All scorings were performed blindly.

Pathway enrichment analysis

Co-expressed genes were determined by having significant positive and negative Pearson correlation coefficient ($p<0.05$) with *DTX1* expression in the CGCI data set. Significance of Pearson correlation was assessed based on the *t* distribution with *n*-2 degrees of freedom as implemented in the R function ”cor.test”. Resulted *p*-values were corrected for multiple testing by the false discovery rate (FDR) method (17), and a corrected *p*-value threshold of *0.05* was used. Pathway enrichment analysis was performed separately on the two sets of genes having significantly positive and negative correlation using ConsensusPathDB webtool (18) with a *p*-value cutoff of *0.01*.

Statistical analyses

A chi-square test was performed to evaluate the differences in the frequency for the prognostic factors. Categorical data were compared using the Fisher’s exact test (two-sided). Survival curves with corresponding *p*-values were calculated using Kaplan-Meier analysis with the log-rank test. In analyses exploiting expression values, a web based cutoff finder tool (http://molpath.charite.de/cutoffanalysis) was used to determine the most prognostic cutoff level for survival outcomes (19). Univariate and multivariate analyses were performed according to the Cox proportional hazards regression model. Progression free survival (PFS) was calculated as a period between the dates of diagnosis and relapse or death from any cause. Otherwise, the patients were censored at the last date of follow-up. Patients in remission were censored at the last date they were known to be alive. Time to progression (TTP) was calculated as a period between the dates of diagnosis and relapse or death from lymphoma. Overall survival (OS) was calculated as a period between the date of diagnosis and the date of death from any cause. Surviving patients were censored at the last date they were known to be alive. P-values less than 0.05 were considered to indicate statistical significance. Data analyses were performed with IBM SPSS Statistics 22.0 (IBM, Armonk, NY, USA).

Supplementary Results

Table S1. Survival associated genes with different variant filtering criteria. Impact of different mutations to protein function was assessed with CADD score.

	dbSNPs removed		Known SNPs removed*		CADD10 Scoring	
	TTP	**OS**	**TTP**	**OS**	**TTP**	**OS**
DTX1	Yes	Yes	Yes	Yes	Yes	Yes
PIM1	No	No	No	Yes	No	Yes
TMSB4X	No	No	No	No	No	Yes
GNA13	No	No	No	No	Yes	No
NOX4	Yes	Yes	Yes	Yes	No	No
AKAP13	No	No	Yes	Yes	No	No
TG	No	No	Yes	Yes	No	No
GSG2	No	No	Yes	Yes	No	No
MDN1	No	No	Yes	Yes	No	No
TMPRSS13	No	No	Yes	Yes	No	No
TMPRSS15	No	No	Yes	Yes	No	No
NEFH	No	No	No	Yes	No	No
CUBN	No	No	No	Yes	No	No
INTS4	No	No	No	Yes	No	No
SLX4IP	No	No	No	Yes	No	No
STT3B	No	No	No	Yes	No	No
GJB7	No	No	No	Yes	No	No
KLHL6	No	No	No	Yes	No	No
KLHL14	No	No	No	Yes	No	No
ITGAE	No	No	Yes	No	No	No
PDE4D	No	No	Yes	No	No	No
NKAPL	No	No	Yes	No	No	No
IL10RB	No	No	Yes	No	No	No
PCDH17	Yes	Yes	No	No	No	No
COL2A1	Yes	Yes	No	No	No	No
COL3A1	Yes	Yes	No	No	No	No
ANKRD36B	Yes	Yes	No	No	No	No
DCTN1	Yes	Yes	No	No	No	No
DPF3	Yes	Yes	No	No	No	No
POLQ	No	Yes	No	No	No	No
MYO9B	No	Yes	No	No	No	No
PRKD2	No	Yes	No	No	No	No
DUSP2	No	Yes	No	No	No	No
TRAPPC9	No	Yes	No	No	No	No
LRRC37A3	No	Yes	No	No	No	No
SPTB	Yes	No	No	No	No	No
CHD1L	Yes	No	No	No	No	No
MYCN	Yes	No	No	No	No	No
PRPF40B	Yes	No	No	No	No	No
*Non-disease causing						

Table S2. Somatic *DTX1* mutations in eight initial screen patients detected automatically and manually from whole exome sequencing alignments.

Gene	Chr	Start	Ref	A	type	AA change
DTX1	12	113495999	T	C	nonsyn SNV	DTX1:NM_004416:exon1:c.T2C:p.M1T
DTX1	12	113496021	G	A	syn SNV	DTX1:NM_004416:exon1:c.G24A:p.G8G,
DTX1	12	113496025	A	C	nonsyn SNV	DTX1:NM_004416:exon1:c.A28C:p.M10L
DTX1	12	113496060	C	T	syn SNV	DTX1:NM_004416:exon1:c.C63T:p.N21N,
DTX1	12	113496087	G	A	stopgain	DTX1:NM_004416:exon1:c.G90A:p.W30X,
DTX1	12	113496150	G	A	syn SNV	DTX1:NM_004416:exon1:c.G153A:p.V51V
DTX1	12	113496151	C	G	nonsyn SNV	DTX1:NM_004416:exon1:c.C154G:p.L52V
DTX1	12	113496201	G	A	syn SNV	DTX1:NM_004416:exon1:c.G204A:p.Q68Q
DTX1	12	113496205	G	A	Nonsyn SNV	DTX1:NM_004416:exon1:c.G208A:p.V70M,
DTX1	12	113515278	GGGCA	G	frameshift deletion	DTX1:NM_004416:exon2:c.310_313del:p.G104fs,
DTX1	12	113515424	A	C	nonsyn SNV	DTX1:NM_004416:exon2:c.A455C:p.Y152S,
DTX1	12	113515433	G	A	nonsyn SNV	DTX1:NM_004416:exon2:c.G464A:p.S155N,

Table S3. *DTX1* mutations in the CGCI cohort detected by RNA sequencing.

Chr.	Ref	Alt	Func.refGene	ExonicFunc.refGene	Exon	CDS	Amino acid change
chr12.113496038	G	C	exonic	nonsyn SNV	exon1	c.G41C	p.G14A
chr12.113496087	G	A	exonic	stopgain SNV	exon1	c.G90A	p.W30X
chr12.113496098	A	C	exonic	nonsyn SNV	exon1	c.A101C	p.H34P
chr12.113496104	G	A	exonic	nonsyn SNV	exon1	c.G107A	p.R36H
chr12.113496115	T	C	exonic	nonsyn SNV	exon1	c.T118C	p.Y40H
chr12.113496144	G	T	exonic	nonsyn SNV	exon1	c.G147T	p.E49D
chr12.113496145	A	T	exonic	nonsyn SNV	exon1	c.A148T	p.N50Y
chr12.113496195	C	G	exonic	nonsyn SNV	exon1	c.C198G	p.D66E
chr12.113496202	C	G	exonic	nonsyn SNV	exon1	c.C205G	p.L69V
chr12.113496234	G	A	exonic	nonsyn SNV	exon1	c.G237A	p.M79I
chr12.113496235	C	A	exonic	nonsyn SNV	exon1	c.C238A	p.H80N
chr12.113515505	T	C	exonic	nonsyn SNV	exon2	c.T536C	p.L179P
chr12.113515723	A	G	exonic	nonsyn SNV	exon2	c.A754G	p.T252A
chr12.113515853	A	C	exonic	nonsyn SNV	exon2	c.A884C	p.N295T
chr12.113515871	G	A	exonic	nonsyn SNV	exon2	c.G902A	p.R301H
chr12.113532926	T	A	exonic	nonsyn SNV	exon7	c.T1466A	p.F489Y

Table S4. WWE1 domain mutations detected in the Nordic cohort by capillary sequencing.

Chr.	mRNA	Ref base	Alt base	Amino acid	Amino acid n.	Ref AA	Alt AA	Type
Chr.12:113 496 049	C388T	C	T	P18S	18	P	S	nonsyn SNV
Chr.12:113 496 050	C389T	C	T	P18L	18	P	L	nonsyn SNV
Chr.12:113 496 064	G403A	G	A	A23T	23	A	T	nonsyn SNV
Chr.12:113 496 070	G409A	G	A	V25M	25	V	M	nonsyn SNV
Chr.12:113 496 071	T410G	T	G	V25G	25	V	G	nonsyn SNV
Chr.12:113 496 073	G412A	G	A	V26M	26	V	M	nonsyn SNV
Chr.12:113 496 076	G415A	G	A	V27M	27	V	M	nonsyn SNV
Chr.12:113 496 086	G425A	G	A	W30X	30	W	X	stopgain SNV
Chr.12:113 496 087	G426A	G	A	W30X	30	W	X	stopgain SNV
Chr.12:113 496 094	G433A	G	A	E33K	33	E	K	nonsyn SNV
Chr.12:113 496 096	G435C	G	C	E33D	33	E	D	nonsyn SNV
Chr.12:113 496 098	A437T	A	T	H34L	34	H	L	nonsyn SNV
Chr.12:113 496 107	G446A	G	A	W37X	37	W	X	stopgain SNV
Chr.12:113 496 108	G447A	G	A	W37X	37	W	X	stopgain SNV
Chr.12:113 496 133	471_472delC	CC	C	H46fs	46	H	fs	Frameshift Deletion
Chr.12:113 496 151	C490G	C	G	L52V	52	L	V	nonsyn SNV
Chr.12:113 496 157	G496A	G	A	E54K	54	E	K	nonsyn SNV
Chr.12:113 496 173	C512T	C	T	S59F	59	S	F	nonsyn SNV
Chr.12:113 496 187	C526T	C	T	Q64X	64	Q	X	stopgain SNV
Chr.12:113 496 190	G529A	G	A	V65M	65	V	M	nonsyn SNV
Chr.12:113 496 202	C541G	C	G	L69V	69	L	V	nonsyn SNV
Chr.12:113 496 203	T542C	T	C	L69P	69	L	P	nonsyn SNV
Chr.12:113 496 205	G544A	G	A	V70M	70	V	M	nonsyn SNV

Chr.12:113 496 212	A551G	A	G	Y72C	72	Y	C	nonsyn SNV
Chr.12:113 496 228	G567C	G	C	Q77H	77	Q	H	nonsyn SNV
Chr.12:113 515 237	C19576T	C	T	R90W	90	R	W	nonsyn SNV
Chr.12:113 515 240	C19579T	C	T	P91S	91	P	S	nonsyn SNV

Table S5. Biological pathways inversely correlated with *DTX1* expression signature.

p-value	q-value	Pathway	Source	Members input_overlap	Members_inputoverlap_gene ids	Size	Effective size
0,0000	0,0238	Allograft Rejection	Wikipathways	IL10; PECR; CASP3; GZMB; IL2RA; CXCL9; CTLA4; IFNG; CXCL11	3002; 4283; 836; 3458; 3559; 3586; 55825; 1493; 6373	80	77
0,0001	0,0238	Fatty Acid Biosynthesis	Wikipathways	ACAA2; PECR; ECHDC3; DECR1; ECHDC1	79746; 55825; 10449; 55862; 1666	22	22
0,0001	0,0238	ifn gamma signaling pathway	BioCarta	IFNG; JAK2; IFNGR1	3459; 3717; 3458	6	5
0,0002	0,0281	Regulation of IFNG signaling	Reactome	IFNG; PTPN2; JAK2; IFNGR1	3459; 5771; 3717; 3458	14	14
0,0002	0,0281	IFN gamma signaling	INOH	IFNG; JAK2; IFNGR1	3459; 3717; 3458	6	6
0,0003	0,0381	Proteasome - Homo sapiens (human)	KEGG	POMP; IFNG; PSMA3; PSMA1; PSMB1; PSMC6	3458; 51371; 5682; 5684; 5689; 5706	44	44
0,0004	0,0381	miR-targeted genes in leukocytes - TarBase	Wikipathways	ANXA2; SNX6; IDH1; CTSC; CD164; ARF4; ACAA2; GOLGA7; ATP6V0E1; LAMTOR3	3417; 1075; 58533; 10449; 378; 302; 51125; 8992; 8763; 8649	152	127
0,0004	0,0381	Proteasome Degradation	Wikipathways	RPN1; IFNG; UBE2D1; PSMA3; PSMA1; PSMC6; PSMB1	5706; 6184; 5689; 5684; 5682; 7321; 3458	64	64
0,0004	0,0381	DroToll-like	INOH	CASP5; CASP3; GZMB; CASP10; PSMA3; PSMA1; PSMB1	5682; 843; 5684; 838; 5689; 836; 3002	65	65
0,0006	0,0467	Interferon gamma signaling	Reactome	IFNG; PTPN2; JAK2; IFNGR1	3459; 5771; 3717; 3458	19	19
0,0011	0,0689	Type II interferon signaling (IFNG)	Wikipathways	CXCL9; IFNG; JAK2; IFNGR1;	3717; 4283; 3458; 3459; 3627	37	37

				CXCL10			
0,0011	0,0689	JAK STAT MolecularVariation 1	INOH	IL2RA; TNFSF10; IL10RB; IFNG; IL15; IL10; JAK2; IFNGR1	3588; 3458; 8743; 3600; 3717; 3559; 3459; 3586	98	97
0,0013	0,0764	Di-unsaturated fatty acid beta-oxidation	EHMN	DBI; ACAA2; DECR1; SLC27A2	11001; 1622; 1666; 10449	23	23
0,0014	0,0764	granzyme a mediated apoptosis pathway	BioCarta	GZMA; GZMB; CASP3	3002; 3001; 836	11	11
0,0015	0,0785	proteasome complex	BioCarta	RPN1; PSMA1; PSMB1; PSMA3	5682; 6184; 5689; 5684	24	24
0,0018	0,0855	RalA downstream regulated genes	Wikipathways	NRAS; YBX3; CDC42	4893; 998; 8531	12	12
0,0019	0,0855	IFN-gamma pathway	PID	IFNG; PTPN2; JAK2; CALM2; IFNGR1	805; 3459; 5771; 3458; 3717	42	42
0,0020	0,0856	IL12-mediated signaling events	PID	IL2RA; GZMA; GZMB; IFNG; B2M; JAK2	3002; 3458; 3559; 3001; 3717; 567	65	62
0,0028	0,1061	Downstream signaling in CD8+ T cells	PID	IL2RA; CALM2; GZMB; IFNG; NRAS; B2M	3559; 805; 3002; 4893; 3458; 567	68	66
0,0028	0,1061	Omega-6 fatty acid metabolism	EHMN	DBI; ACAA2; DECR1; SLC27A2	11001; 1666; 10449; 1622	28	28
0,0029	0,1072	chaperones modulate interferon signaling pathway	BioCarta	IFNG; JAK2; IFNGR1	3459; 3717; 3458	15	14
0,0032	0,1073	Calcium signaling in the CD4+ TCR pathway	PID	IFNG; IL2RA; CALM2; AKAP5	3559; 3458; 9495; 805	29	29
0,0032	0,1073	Interferon Signaling	Reactome	EIF4E3; IFNG; DDX58; JAK2; IFNGR1; PTPN2	317649; 3459; 3458; 5771; 23586; 3717	68	68
0,0034	0,1099	Calcineurin-regulated NFAT-dependent transcription in lymphocytes	PID	IFNG; IL2RA; CALM2; CASP3; CTLA4	3559; 805; 3458; 836; 1493	49	48

Table S6. Biological pathways associated with *DTX1* expression signature.

p-value	q-value	Pathway	Source	Members_input overlap	Members_inputo verlap_gene ids	Size	Effect ive_si ze
0,0000	0,0000	Chromatin modifying enzymes	Reacto me	HDAC1; KDM1A; NCOR2; MCRS1; SETD1A; RCOR1; EP400; AEBP2; SMARCA4; JADE2; SAP130; EHMT1; CHD3; GPS2; JMJD6; CHD4; HCFC1; USP22; BRPF3; KDM4B; BRPF1; DMAP1; KDM6B; DOT1L; MTA1; HMG20B; MTA3; KMT2C; KMT2B; KMT2A; SMARCB1; SMARCC2; KMT2D; KANSL1; TRRAP; SETD8; EHMT2; SMARCD2; SMARCD1; HDAC10; ING5; EP300; SETD7; KAT8; KDM2B; TAF6L; WHSC1; ARID1A; KANSL3; KAT5; SETDB1; YEATS2; MBD3; GATAD2B; KDM3B; KAT6B; GATAD2A; PHF2; KDM5A; TADA3; KDM5C	9869; 3065; 79595; 8085; 9739; 387893; 8289; 9112; 10524; 23030; 57634; 1107; 6602; 6598; 84444; 7862; 23522; 58508; 79813; 23135; 10474; 80854; 9757; 121536; 10445; 51780; 5253; 2033; 1108; 8295; 23028; 53615; 6597; 4297; 3054; 5927; 84148; 10362; 23186; 23338; 6603; 6601; 55689; 284058; 84678; 8242; 55929; 23326; 55683; 57504; 2874; 84289; 57459; 23210; 7468; 10919; 27154; 9612; 10629; 54815; 83933	253	249
0,0000	0,0000	Chromatin organization	Reacto me	HDAC1; KDM1A; NCOR2; MCRS1; SETD1A; RCOR1;	9869; 3065; 79595; 8085; 9739; 387893;	253	249

				EP400; AEBP2; SMARCA4; JADE2; SAP130; EHMT1; CHD3; GPS2; JMJD6; CHD4; HCFC1; USP22; BRPF3; KDM4B; BRPF1; DMAP1; KDM6B; DOT1L; MTA1; HMG20B; MTA3; KMT2C; KMT2B; KMT2A; SMARCB1; SMARCC2; KMT2D; KANSL1; TRRAP; SETD8; EHMT2; SMARCD2; SMARCD1; HDAC10; ING5; EP300; SETD7; KAT8; KDM2B; TAF6L; WHSC1; ARID1A; KANSL3; KAT5; SETDB1; YEATS2; MBD3; GATAD2B; KDM3B; KAT6B; GATAD2A; PHF2; KDM5A; TADA3; KDM5C	8289; 9112; 10524; 23030; 57634; 1107; 6602; 6598; 84444; 7862; 23522; 58508; 79813; 23135; 10474; 80854; 9757; 121536; 10445; 51780; 5253; 2033; 1108; 8295; 23028; 53615; 6597; 4297; 3054; 5927; 84148; 10362; 23186; 23338; 6603; 6601; 55689; 284058; 84678; 8242; 55929; 23326; 55683; 57504; 2874; 84289; 57459; 23210; 7468; 10919; 27154; 9612; 10629; 54815; 83933		
0,0000	0,0014	Insulin Signaling	Wikipathways	MAP4K1; MAP4K2; MAP4K4; MAP2K3; MAP2K2; FOXO1; MAP2K7; TSC2; MINK1; MAP3K9; INPPL1; EGR1; PIK3CG; PFKM; PFKL; MAPK7;	50488; 5580; 10603; 11184; 1958; 6844; 5598; 9265; 5605; 5606; 5602; 5609; 2308; 6513; 7249; 3551; 5578; 4294; 4296; 4293; 5871; 3636; 6812; 5294; 5213; 5211; 115703; 207; 9448; 208; 6464	160	160

				STXBP1; SHC1; PRKCA; PRKCD; SH2B2; CYTH3; IKBKB; VAMP2; AKT1; AKT2; SLC2A1; MAP3K10; MAP3K11; ARHGAP33; MAPK10			
0,0000	0,0027	Regulation of cholesterol biosynthesis by SREBP (SREBF)	Reacto me	NFYC; ACACB; TM7SF2; MBTPS1; KPNB1; SREBF2; SREBF1; MVD; LSS; FASN; MVK	4597; 4047; 6720; 3837; 6721; 8720; 7108; 32; 4598; 2194; 4802	29	29
0,0000	0,0027	Lysine degradation - Homo sapiens (human)	KEGG	KMT2C; KMT2B; PHYKPL; EHMT2; KMT2D; WHSC1; KMT2A; EHMT1; SETD1A; SETD8; SUV420H2; DOT1L; ASH1L; SETDB1; SETD7	80854; 9739; 9869; 85007; 58508; 8085; 4297; 9757; 7468; 84787; 387893; 55870; 79813; 84444; 10919	52	52
0,0000	0,0033	chromatin remodeling by hswi/snf atp-dependent complexes	BioCart a	SMARCC2; GTF2F1; NF1; ARID1A; POLR2A; SMARCD1; SMARCB1; SMARCA4	8289; 4763; 6598; 2962; 6597; 6602; 5430; 6601	16	16
0,0000	0,0051	VEGF	INOH	MAP4K2; IKBKB; MAP2K2; PLCG1; MAPK10; ADRBK1; MAP3K9; MAP3K11; GRK5; CSNK1D; MAPK7; WEE1; PRKAB1; PRKCA; CAMK2G; PRKCE; PRKCD; CSNK1G2;	207; 5578; 5606; 818; 2869; 5605; 5580; 4233; 2260; 5602; 1453; 5566; 3710; 208; 156; 3932; 5335; 3551; 1018; 10298; 5564; 4294; 7465; 5871; 4293; 5581; 5598; 4296; 5609; 1455; 1025; 5575	187	185

				PRKAR1B; CDK9; ITPR3; FGFR1; MAP2K3; AKT1; AKT2; MAP3K10; MET; CDK3; PRKACA; PAK4; MAP2K7; LCK			
0,0000	0,0090	EPO signaling	INOH	MAP4K2; IKBKB; MAP2K2; AKT2; MAPK10; ADRBK1; MAP3K9; MAP3K11; GRK5; CSNK1D; MAPK7; WEE1; PRKAB1; PRKCA; CAMK2G; PRKCE; PRKCD; CSNK1G2; PRKAR1B; CDK9; FGFR1; EPOR; MAP2K3; AKT1; MAP3K10; MET; CDK3; PRKACA; PAK4; MAP2K7; LCK	207; 5578; 5606; 818; 2869; 5605; 5580; 4233; 2260; 5602; 1453; 5566; 208; 2057; 156; 3932; 3551; 1018; 10298; 5564; 4294; 7465; 5871; 4293; 5581; 5598; 4296; 5609; 1455; 1025; 5575	185	183
0,0001	0,0101	Activation of gene expression by SREBF (SREBP)	Reacto me	NFYC; TM7SF2; ACACB; SREBF2; SREBF1; MVD; LSS; FASN; MVK	4597; 4047; 6720; 32; 6721; 7108; 4598; 2194; 4802	24	24
0,0001	0,0101	Signaling Pathways in Glioblastoma	Wikipat hways	MET; TP53; PIK3C2B; AKT1; PRKCA; PRKCD; FOXO1; MSH6; PIK3CG; MAP2K3; MAP2K2; PLCG1; MAP2K7; NF1; EP300; TSC2; FGFR1; AKT2	5294; 2956; 5605; 4763; 5606; 5335; 7249; 5609; 2308; 5580; 7157; 2033; 208; 2260; 207; 5287; 4233; 5578	83	82
0,0001	0,0101	Factors involved in megakaryocyte development and	Reacto me	HDAC1; KDM1A; DOCK2; ZFPM1; DOCK6; KIF26A;	8165; 3065; 3831; 1794; 7157; 26153; 5566;	114	113

		platelet production		RCOR1; MAFK; CBX5; WEE1; CABLES2; HMG20B; SH2B2; PRKAR1B; SH2B1; KIFC1; TP53; AKAP1; PRKACA; KLC1; KLC2; KLC4	3833; 23028; 64837; 89953; 23468; 7975; 25970; 10362; 23186; 10603; 81928; 7465; 161882; 5575; 57572		
0,0001	0,0101	telomeres telomerase cellular aging and immortality	BioCarta	TNKS; TP53; PRKCA; AKT1; POLR2A; PPP2R5D; TERT	7157; 207; 5528; 7015; 8658; 5578; 5430	15	15
0,0001	0,0101	Histone Modifications	Wikipathways	EHMT1; KMT2C; ASH1L; EHMT2; KMT2D; KMT2A; SETD1A; SETD8; SETD7; AEBP2; DOT1L; SETDB1; SUV420H2	84787; 9739; 84444; 55870; 121536; 387893; 10919; 9869; 8085; 79813; 4297; 58508; 80854	49	49
0,0001	0,0101	Signaling events mediated by HDAC Class I	PID	HDAC1; SMG5; CHD3; EP300; CHD4; ZFPM1; RANGAP1; SMURF1; PRKACA; MBD3; GATAD2B; GATAD2A; SIN3B; NCOR2	23309; 3065; 5905; 57459; 9612; 5566; 1108; 23381; 161882; 53615; 1107; 54815; 2033; 57154	56	56
0,0001	0,0101	Fc gamma R-mediated phagocytosis - Homo sapiens (human)	KEGG	MARCKSL1; LIMK2; INPP5D; INPPL1; DOCK2; PRKCD; LIMK1; PRKCE; PLCG1; PIK3CG; PLA2G6; AKT1; AKT2; PRKCA; PIP5K1C; DNM2; ASAP3; WAS; GSN	3635; 3636; 65108; 5294; 2934; 8398; 207; 208; 5335; 1785; 1794; 7454; 55616; 23396; 3984; 3985; 5578; 5580; 5581	92	92
0,0001	0,0101	IL-7 signaling	INOH	MAP4K2; IKBKB; MAP2K2; AKT2; MAPK10; ADRBK1;	207; 5578; 5606; 818; 2869; 5605; 5580; 4233; 2260; 5602; 1453; 5566;	184	182

				MAP3K9; MAP3K11; GRK5; CSNK1D; MAPK7; WEE1; PRKAB1; PRKCA; CAMK2G; PRKCE; PRKCD; CSNK1G2; PRKAR1B; CDK9; FGFR1; MAP2K3; AKT1; MAP3K10; MET; CDK3; PRKACA; PAK4; MAP2K7; LCK	208; 156; 3932; 3551; 1018; 10298; 5564; 4294; 7465; 5871; 4293; 5581; 5598; 4296; 5609; 1455; 1025; 5575		
0,0001	0,0119	WNT-Core	Signalink	FZD1; TCF3; AXIN1; FZD8; SMAD3; DVL2; AKT1; CSNK1D; HNF1A; PRKACA; APC2; DVL1	8321; 8325; 6927; 6929; 8312; 1453; 5566; 1855; 1856; 207; 10297; 4088	44	44
0,0001	0,0125	Regulation of Androgen receptor activity	PID	HDAC1; EHMT2; HDAC7; TRIM24; EGR1; PDE9A; RXRB; KAT5; PKN1; FOXO1; ZMIZ2; EP300; POU2F1	51564; 3065; 2308; 5152; 83637; 10919; 8805; 5585; 10524; 2033; 1958; 6257; 5451	51	51
0,0001	0,0125	AndrogenReceptor	NetPath	HDAC1; HDAC7; SF1; AKT1; NCOR2; GSN; NONO; CDC37; PXN; DAPK3; CDC25B; PARP1; SMAD3; PELP1; CDK9; PATZ1; EP300; GTF2F1; WHSC1; CCND3; KAT5; PIAS3; PIAS4; ZMIZ2; ZMIZ1	23598; 207; 3065; 7536; 10401; 5829; 10524; 2962; 51564; 11140; 994; 4088; 83637; 57178; 2934; 4841; 2033; 896; 27043; 1613; 51588; 9612; 7468; 142; 1025	143	143
0,0001	0,0130	Diseases of signal transduction	Reactome	HDAC1; TGFB1; HDAC7; HDAC6; SMAD3;	207; 3065; 1523; 23493; 6464; 11064; 399687;	180	178

				MYO18A; AKT2; TSC2; NCOR2; HEYL; MAML1; CDC37; SYVN1; OS9; SHC1; TRIM24; TNKS; CUX1; HDAC10; EP300; HEY2; FGFR1; AKT1; FOXO1; PLCG1; CASP9; HES1; CNTRL; LCK	9794; 2260; 51564; 11140; 842; 4088; 5335; 7249; 8805; 208; 2033; 7040; 2308; 84447; 3932; 8658; 10956; 26508; 3280; 10013; 9612; 83933		
0,0002	0,0157	B Cell Receptor Signaling Pathway	Wikipathways	MAP4K1; BCL6; INPP5D; SHC1; PIP5K1C; AKT1; CD81; CD22; PRKCD; PLCG1; PIK3CG; IKBKB; MAP2K2; FOXO1; PTPN18; MEF2D; GTF2I; LCK; CD79A	2969; 5580; 933; 11184; 5605; 2308; 3551; 5335; 975; 973; 23396; 4209; 604; 5294; 3635; 207; 3932; 26469; 6464	98	97
0,0002	0,0163	EGFR1	NetPath	HDAC1; KHDRBS1; JUND; FRS3; SMAD3; MAP2K3; MAP2K2; FOXO1; CC2D1A; APLP2; HIP1; ADRBK1; GSN; MINK1; DLG3; PHLPP1; ARAP1; PIAS3; ARHGEF7; MYH9; PIK3CG; MPRIP; TRIM24; PXN; MAPK7; EPHB2; SHC1; EPHB4; PTPN23; PRKCA; EPN1; MAP2K7; VCL; PRKCD; LPP; PIK3C2B; SFPQ; SH2B1; ALDOA;	207; 5578; 334; 3092; 5605; 23294; 2048; 26469; 156; 2934; 1487; 10401; 9564; 54862; 5829; 2050; 5580; 4088; 4026; 4233; 116985; 2308; 3932; 5294; 5287; 5598; 8874; 57513; 3065; 7157; 842; 6421; 1741; 3727; 25970; 4627; 6464; 23164; 5609; 3636; 10657; 5606; 55616; 10188; 50488; 23513; 25930; 10817; 28964; 23239; 5335; 9146; 7414;	453	448

				HGS; ANKS1A; BCAR1; TNK2; PTPN18; TP53; INPPL1; AKT1; PLCG1; CASP9; SCRIB; MET; CASKIN2; GIT1; CTBP1; ATXN2; LCK; ASAP3	226; 6311; 8805; 29924		
0,0002	0,0163	DAG and IP3 signaling	Reacto me	ADCY6; PRKCA; PRKCE; ADCY9; PRKCD; PLCG1; PRKACA; PRKAR1B; ITPR3; ADRBK1	112; 5578; 5335; 115; 5566; 5581; 156; 5580; 5575; 3710	34	34
0,0002	0,0163	Insulin signaling pathway - Homo sapiens (human)	KEGG	MKNK2; IKBKB; AKT1; FOXO1; MAPK10; TSC2; RPTOR; PPP1R3F; INPPL1; PRKAB1; PIK3CG; FASN; PHKG2; ACACA; SHC1; ACACB; PHKA2; SH2B2; PRKAR1B; EXOC7; MAP2K2; AKT2; SREBF1; PRKACA	31; 32; 3636; 6720; 7249; 5256; 5261; 2194; 5294; 57521; 89801; 207; 208; 23265; 2308; 2872; 3551; 6464; 10603; 5564; 5566; 5575; 5602; 5605	140	139
0,0002	0,0167	VEGF Signaling Pathway	Pharm GKB	MAP2K3; TIMP3; AKT1; PRKCA; PRKCE; PRKCD; PLCG1; MAP2K2; PIK3C2B; AKT2; MAPK10; MAPK7; MAP2K7; FGFR1	7078; 5287; 5578; 5580; 5581; 207; 208; 5335; 5598; 5602; 5605; 5606; 5609; 2260	61	61
0,0003	0,0178	Hedgehog signaling events mediated by Gli proteins	PID	HDAC1; SMO; GLI2; IFT172; PRKCD; CSNK1G2; AKT1; CSNK1D;	207; 23309; 3065; 27148; 1453; 5566; 5727; 26160; 1455; 5580; 6608; 2736	49	48

				PRKACA; STK36; PTCH1; SIN3B			
0,0003	0,0178	Notch-mediated HES/HEY network	PID	HDAC1; KDM1A; TCF3; MAML1; PARP1; SPEN; HES1; CTBP1; EP300; HEY2; NCOR2; HES6	3065; 6929; 55502; 1487; 9612; 23028; 23013; 23493; 142; 3280; 2033; 9794	48	48
0,0003	0,0178	Notch signaling pathway - Homo sapiens (human)	KEGG	HDAC1; EP300; DTX2; MAML1; NOTCH4; DVL2; DVL1; CTBP1; RFNG; HES1; NCOR2; NUMBL	9612; 9253; 1855; 1856; 9794; 5986; 1487; 3280; 113878; 3065; 2033; 4855	48	48
0,0003	0,0194	Syndecan-1-mediated signaling events	PID	TGFB1; LAMA5; COL11A2; MET; COL5A1; PRKACA; COL4A1; COL1A1; COL6A1; COL1A2; FGFR1	2260; 7040; 5566; 1291; 1282; 1277; 3911; 1278; 1302; 4233; 1289	43	42
0,0003	0,0194	Signaling by PDGF	Reacto me	PPP2R1A; PRKAR1B; SPTAN1; FRS3; SPRED3; MAP2K2; PLCG1; RASAL1; TSC2; ADRBK1; STAT6; NF1; RASA3; PDGFD; SHC1; PRKCA; DAB2IP; CAMK2G; VCL; PRKCD; FOXO1; SYNGAP1; PPP2R5D; AKT2; COL4A2; COL4A1; ITPR3; PHLPP1; BCAR1; FGFR1; ADCY6; PRKCE; AKT1; ADCY9; CASP9; MAP3K11; PRKACA;	207; 22821; 5578; 115; 5566; 6464; 5605; 8831; 5580; 399473; 2260; 818; 9564; 842; 10817; 5335; 1282; 7249; 156; 5518; 26523; 23239; 3710; 208; 1284; 112; 3932; 1291; 6709; 7414; 6778; 8437; 2308; 80310; 153090; 5528; 5581; 4296; 4763; 5575; 5526	301	298

				COL6A1; AGO1; LCK; PPP2R5B			
0,0003	0,0194	Signaling by EGFR	Reacto me	PPP2R1A; SPTAN1; FRS3; SPRED3; MAP2K2; PLCG1; EPN1; RASAL1; TSC2; ADRBK1; ADAM12; ARHGEF7; PXN; NF1; RASA3; SHC1; PRKCA; DAB2IP; CAMK2G; VCL; PRKCD; FOXO1; HGS; SYNGAP1; AKT2; PRKAR1B; ITPR3; PHLPP1; FGFR1; ADCY6; PRKCE; AKT1; ADCY9; CASP9; MAP3K11; PRKACA; PPP2R5D; AGO1; LCK; PPP2R5B	207; 22821; 5578; 115; 6464; 5605; 8831; 2308; 5580; 399473; 2260; 818; 842; 10817; 8038; 5335; 5566; 5829; 7249; 156; 5518; 26523; 23239; 3710; 208; 112; 3932; 9146; 8874; 7414; 8437; 6709; 153090; 5528; 5581; 4296; 4763; 5575; 29924; 5526	292	289
0,0003	0,0194	EGFR interacts with phospholipase C-gamma	Reacto me	ADCY6; PRKCA; PRKCE; ADCY9; PRKCD; PLCG1; PRKACA; PRKAR1B; ITPR3; ADRBK1	112; 5578; 5335; 115; 5566; 5581; 156; 5580; 5575; 3710	36	36
0,0003	0,0194	PLC-gamma1 signalling	Reacto me	ADCY6; PRKCA; PRKCE; ADCY9; PRKCD; PLCG1; PRKACA; PRKAR1B; ITPR3; ADRBK1	112; 5578; 5335; 115; 5566; 5581; 156; 5580; 5575; 3710	36	36
0,0004	0,0207	Thyroid hormone signaling pathway - Homo sapiens (human)	KEGG	HDAC1; PLCG1; EP300; TP53; SLC9A1; MAP2K2; NOTCH4; PRKCA;	7249; 6257; 9862; 5294; 207; 208; 5335; 4855; 2308; 10025; 842; 6513; 6548; 6567; 5566; 5578; 478; 5605;	119	119

				SLC16A2; MED24; RXRB; PIK3CG; AKT1; AKT2; PRKACA; SLC2A1; MED16; FOXO1; ATP1A3; CASP9; TSC2	2033; 7157; 3065		
0,0004	0,0222	PLCG1 events in ERBB2 signaling	Reacto me	ADCY6; PRKCA; PRKCE; ADCY9; PRKCD; PLCG1; PRKACA; PRKAR1B; ITPR3; ADRBK1	112; 5578; 5335; 115; 5566; 5581; 156; 5580; 5575; 3710	37	37
0,0004	0,0222	EGF-Core	Signalin k	MAP4K1; MINK1; MAP3K9; MAP4K4; MAP2K2; MKNK2; GRAP; PIK3CG; MAP3K10; MAP3K11; MAP2K3; MAP4K2; MAPK10; MAPK7; MAP2K7; SMAD3; TAOK1; TAOK2; SHC1	9344; 5294; 4293; 4294; 4296; 57551; 9448; 5871; 5598; 2872; 6464; 50488; 5606; 11184; 5602; 5605; 5609; 4088; 10750	105	104
0,0005	0,0222	Signalling by NGF	Reacto me	HDAC1; PPP2R1A; SPTAN1; FRS3; SPRED3; IKBKB; MAP2K2; FOXO1; DNM2; ARHGAP4; TSC2; ADRBK1; RASAL1; ARHGEF7; ARHGEF2; ARHGEF1; ADCY9; MAPK7; NF1; ARHGDIA; FGFR1; FGD1;	207; 5578; 5605; 9500; 156; 208; 1785; 11108; 5528; 4763; 3065; 22821; 8831; 29; 26523; 3710; 2308; 112; 3932; 3551; 2245; 5598; 8874; 9181; 9138; 7414; 5580; 842; 835; 5518; 6709; 393; 8437; 4296; 5575; 6464; 2260; 10817; 5566; 399473; 7249;	386	382

				SHC1; PRKCA; DAB2IP; CAMK2G; VCL; PRKCD; SYNGAP1; ABR; PRKAR1B; ITPR3; PHLPP1; RASA3; ADCY6; PRKCE; CASP2; AKT1; MAGED1; AKT2; PLCG1; CASP9; PRDM4; MAP3K11; PRKACA; PPP2R5D; AGO1; LCK; PPP2R5B	23239; 5335; 818; 396; 115; 153090; 5581; 5526		
0,0005	0,0222	Aurora A signaling	PID	FZR1; TP53; CDC25B; TACC3; AKT1; PRKACA; GIT1; ARHGEF7; PPP2R5D	7157; 207; 10460; 994; 5566; 28964; 51343; 5528; 8874	31	31
0,0005	0,0222	TGF_beta_Receptor	NetPath	HDAC1; MAP4K1; TGFB1; TRIM33; JUND; SMAD3; MAP2K3; AKT1; FOXO1; SOX9; SMURF1; ANAPC2; IRF2BP1; PXN; STK11IP; ENG; KPNB1; HGS; PRKAR1B; EP300; BCAR1; NFYC; E2F4; TP53; TAB1; FZR1; CTCF	207; 51592; 29882; 2022; 3065; 10664; 7157; 3837; 4088; 11184; 2033; 5606; 7040; 2308; 9564; 9146; 51343; 6662; 57154; 26145; 3727; 114790; 1874; 5829; 10454; 5575; 4802	174	173
0,0005	0,0222	SUMOylation of DNA damage response and repair proteins	Reactome	AAAS; MDC1; POM121; HDAC7; XPC; PHC2; PARP1; RING1; NUP188; HERC2; RAD52; PIAS4; CBX8;	7508; 51564; 51588; 8924; 8535; 57332; 1912; 23511; 5893; 6015; 22955; 142; 9883; 9656; 8086	74	73

				CBX4; SCMH1			
0,0005	0,0222	SUMO E3 ligases SUMOylate target proteins	Reactome	AAAS; MDC1; POM121; HDAC7; XPC; PHC2; PARP1; RING1; NUP188; HERC2; RAD52; PIAS4; CBX8; CBX4; SCMH1	7508; 51564; 51588; 8924; 8535; 57332; 1912; 23511; 5893; 6015; 22955; 142; 9883; 9656; 8086	74	73
0,0005	0,0227	Signaling events mediated by Hepatocyte Growth Factor Receptor (c-Met)	PID	RPTOR; EGR1; INPP5D; SHC1; INPPL1; MAP2K2; KPNB1; HGS; AKT2; AKT1; PLCG1; PXN; PAK4; RANBP10; BCAR1; MET	9564; 3837; 5335; 207; 57521; 6464; 10298; 5829; 5605; 57610; 1958; 3635; 9146; 208; 3636; 4233	82	81
0,0006	0,0233	TCR	NetPath	MAP4K1; EGR1; EVL; HDAC7; DOCK2; GRAPL; KHDRBS1; IKBKB; MAP2K2; PLCG1; DNM2; DIAPH1; PI4KA; GRAP; ARHGEF7; CD82; ARHGEF2; PXN; ATP1A3; FCRL3; MAPK7; SHC1; PRKCD; HGS; PIK3C2B; SLAMF6; WAS; SNRNP70; INPP5D; AKT1; CASKIN2; STK39; WIPF1; LCK	207; 10657; 6625; 57513; 3732; 5829; 6464; 5605; 5580; 1729; 51564; 5335; 1794; 11184; 478; 3635; 1785; 3932; 7456; 3551; 5297; 115352; 1958; 10750; 9146; 27347; 7454; 400581; 114836; 5287; 5598; 51466; 8874; 9181	244	239
0,0006	0,0233	MAPK Signaling Pathway	Wikipathways	MAP4K1; TGFB1; MAP4K4; JUND; MAP2K3; MAP2K2; AKT2;	50488; 10454; 5580; 994; 11184; 5598; 23162; 5605; 5606; 5609; 835; 5566; 2260;	168	166

				MAP2K7; MINK1; MAPK7; NF1; MAPK8IP3; CDC25B; PRKCD; TP53; TAOK1; TAOK2; FGFR1; IKBKB; CASP2; AKT1; TAB1; CASP9; MAP3K11; PRKACA; MAPK10	3551; 4296; 7157; 57551; 3727; 842; 9344; 5602; 4763; 207; 9448; 208; 7040		
0,0006	0,0233	Fibroblast growth factor-1	NetPath	DLG3; PTPN18; SHC1; INPPL1; MAP2K2; SLC7A6; HGS; PRKCD; AKT1; PLCG1; TMEM63B; MAPK7; AP1B1; FGFR1; TPCN1	2260; 207; 5335; 9146; 53373; 6464; 9057; 1741; 5598; 26469; 162; 3636; 5580; 5605; 55362	74	74
0,0006	0,0233	RhoA signaling pathway	PID	DIAPH1; LIMK2; LIMK1; VCL; MKL1; EZR; MAP2K3; PKN1; PIP5K1C; CIT; SLC9A1	3985; 1729; 5606; 3984; 57591; 6548; 7430; 5585; 7414; 11113; 23396	45	45
0,0006	0,0233	Notch Signaling Pathway	Wikipathways	HDAC1; DTX2; MAML1; NOTCH4; DVL2; DVL1; RFNG; CTBP1; HES1; NCOR2; NUMBL	9612; 113878; 1487; 3065; 5986; 1855; 1856; 9253; 3280; 9794; 4855	45	45
0,0007	0,0258	Integrin	INOH	COL18A1; SHC1; COL11A2; GPC1; DOCK2; DOCK6; VCL; BGN; AGRN; MAP2K2; ITGA11; COL1A2; COL4A2; COL4A1; COL1A1; COL6A1; COL16A1;	6464; 5605; 1278; 1282; 1302; 3932; 1277; 1794; 80781; 1284; 22801; 9564; 2817; 375790; 1291; 7414; 1307; 633; 5829; 57572; 1289	124	124

				COL5A1; BCAR1; LCK; PXN			
0,0007	0,0258	mRNA surveillance pathway - Homo sapiens (human)	KEGG	SMG5; PPP2R1A; SMG7; SMG6; NXF1; SYMPK; DAZAP1; SRRM1; ACIN1; CASC3; PPP2R3B; CPSF7; UPF1; PPP2R5B; PNN; PPP2R5D; CPSF1	10250; 28227; 9887; 29894; 10482; 23293; 22794; 5411; 23381; 5976; 5518; 5526; 5528; 26528; 22985; 79869; 8189	91	91
0,0008	0,0296	Notch Signaling Pathway	Wikipathways	HDAC1; MAML1; NOTCH4; RING1; LCK; SPEN; AKT1; HES1; EP300; HEY2; NCOR2; HES6; NUMBL	3065; 9612; 23013; 2033; 207; 9253; 23493; 3932; 3280; 6015; 55502; 9794; 4855	61	61

Figure S1. Mutational landscape of the Nordic cohort of DLBCLs with clinically high risk disease. Types of mutations and their proportion among all recorded mutations in the initial exome sequencing screening cohort. The most common type of mutation (710/922) was non-synonymous single nucleotide variation (SNV). Four of the non-synonymous SNVs occurred in more than one patient. Two recurrent specific amino acid changes were identified, one occurring in two patients and the other in three. The relative frequencies of different types of mutations were similar between relapsed and non-relapsed cases. On average, tumors harbored 115 SNVs and the samples from the patients who relapsed presented higher number of SNVs than the patients without relapse (mean of 135 compared to 96, *p=ns*). A detailed list of the somatic variants detected in the screen is available on request.

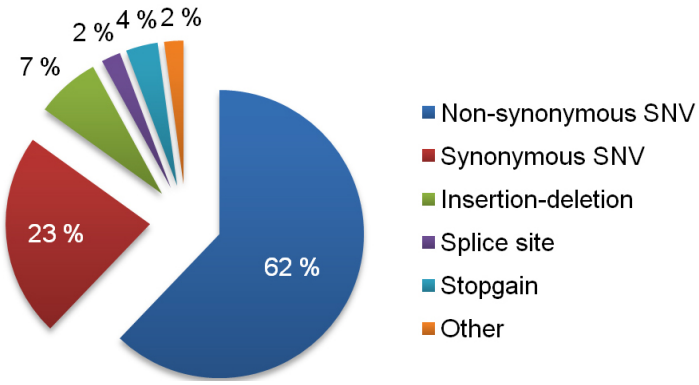

Figure S2. Immunohistochemical staining pattern of DTX1 in DLBCL and gene expression profile according to *DTX1* expression. Immunohistochemical staining of DTX1 was carried out using reactive lymph node and tonsil and DLBCL tissue from 30 patients included in the Nordic cohort. (A) *DTX1* expression in normal lymph node. (B) DLBCL sample with wild-type WWE1 domain and high *DTX1* expression. (C) DLBCL sample with E33D missense mutation of *DTX1* and low expression. (D) DTX1 protein levels in association with WWE1 domain mutations of *DTX1*. Boxes contain expression values between the 25th and 75th percentiles. (E) *DTX1* expression in association with *DTX1* mutations. Boxes contain expression values between the 25th and 75th percentiles. (F) Gene expression profile according to *DTX1* expression. Heat map shows clustering of the genes based on positive or negative correlation with *DTX1* expression. Color changes within the row indicate expression relative to the average of all samples. Red indicate high expression, blue indicate low expression.

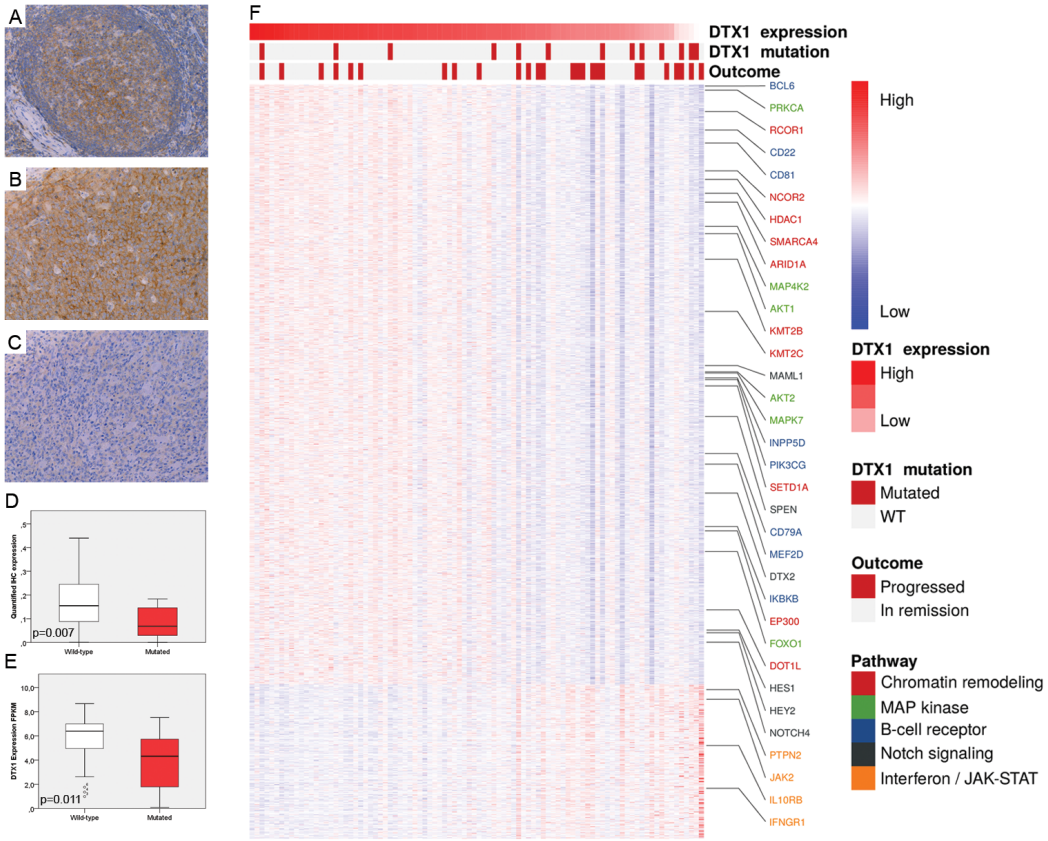

References

1. Holte H, Leppa S, Bjorkholm M, et al. Dose-densified chemoimmunotherapy followed by systemic central nervous system prophylaxis for younger high-risk diffuse large B-cell/follicular grade 3 lymphoma patients: results of a phase II Nordic Lymphoma Group study. Ann Oncol. 2013;24(5):1385-1392.
2. Morin RD, Mendez-Lago M, Mungall AJ, et al. Frequent mutation of histone-modifying genes in non-Hodgkin lymphoma. Nature. 2011;476(7360):298-303.
3. Morin RD, Mungall K, Pleasance E, et al. Mutational and structural analysis of diffuse large B-cell lymphoma using whole-genome sequencing. Blood. 2013;122(7):1256-1265.
4. Lenz G, Wright G, Dave SS, et al. Stromal gene signatures in large-B-cell lymphomas. N Engl J Med. 2008;359(22):2313-2323.
5. Li H, Durbin R. Fast and accurate short read alignment with Burrows-Wheeler transform. Bioinformatics. 2009;25(14):1754-1760.
6. Li H. A statistical framework for SNP calling, mutation discovery, association mapping and population genetical parameter estimation from sequencing data. Bioinformatics. 2011;27(21):2987-2993.
7. Koboldt DC, Zhang Q, Larson DE, et al. VarScan 2: somatic mutation and copy number alteration discovery in cancer by exome sequencing. Genome Res. 2012;22(3):568-576.
8. Wang K, Li M, Hakonarson H. ANNOVAR: functional annotation of genetic variants from high-throughput sequencing data. Nucleic Acids Res. 2010;38(16):e164.
9. Andrews S. FastQC: A quality control tool for high throughput sequence data.
10. Bolger AM, Lohse M, Usadel B. Trimmomatic: a flexible trimmer for Illumina sequence data. Bioinformatics. 2014;30(15):2114-2120.
11. Kim D, Pertea G, Trapnell C, et al. TopHat2: accurate alignment of transcriptomes in the presence of insertions, deletions and gene fusions. Genome biology. 2013;14(4):R36.

12. Trapnell C, Roberts A, Goff L, et al. Differential gene and transcript expression analysis of RNA-seq experiments with TopHat and Cufflinks. Nature protocols. 2012;7(3):562-578.
13. Edmonson MN, Zhang J, Yan C, et al. Bambino: a variant detector and alignment viewer for next-generation sequencing data in the SAM/BAM format. Bioinformatics. 2011;27(6):865-866.
14. Kircher M, Witten DM, Jain P, et al. A general framework for estimating the relative pathogenicity of human genetic variants. Nat Genet. 2014;46(3):310-315.
15. Schwarz JM, Rodelsperger C, Schuelke M, Seelow D. MutationTaster evaluates disease-causing potential of sequence alterations. Nat Methods. 2010;7(8):575-576.
16. Rantanen V, Valori M, Hautaniemi S. Anima: modular workflow system for comprehensive image data analysis. Front Bioeng Biotechnol. 2014;2:25.
17. Benjamini Y, Hochberg Y. Controlling false discovery rate: A practical and powerful approach to multiple testing. Journal of the Royal Statistical Society Series B (Methodological). 1995;57(1):289-300.
18. Kamburov A, Pentchev K, Galicka H, et al. ConsensusPathDB: toward a more complete picture of cell biology. Nucleic Acids Res. 2011;39(Database issue):D712-717.
19. Budczies J, Klauschen F, Sinn BV, et al. Cutoff Finder: a comprehensive and straightforward Web application enabling rapid biomarker cutoff optimization. PLoS One. 2012;7(12):e51862.